Science in China Series E: Technological Sciences

www.scichina.com
tech.scichina.com
www.springerlink.com

Variability of complementary relationship and its mechanism on different time scales

YANG HanBo†, YANG DaWen†, LEI ZhiDong, SUN FuBao & CONG ZhenTao

State Key Laboratory of Hydro-Science and Engineering, Department of Hydraulic Engineering, Tsinghua University, Beijing 100084, China

In the complementary relationship (CR) between actual and potential evapotranspiration, wet environment evapotranspiration (E_w) is usually calculated using the Priestley-Taylor (P-T) equation. Based on the data obtained from 38 catchments of the Haihe River basin and the Weishan experiment site in Shandong Province of China, this study has found variations in the Priestley-Taylor parameter α (e.g. increase in values with increase in the amount of precipitation on annual scale, seasonal fluctuation noted to be at a maximum during winter and at a minimum during summer, and increased values in the forenoon and decreased values in the afternoon on an hourly scale). This paper explains that the inter-annual variation in α is due to the negative feedback of atmosphere in response to changes in actual increase in evapotranspiration, which is weakened because the atmosphere system is open. The parameter α undergoes a seasonal fluctuation brought about by seasonal changes in advection between continent and ocean; α likewise undergoes a daily variation as a result of atmospheric hysteresis in response to the changes in land surface energy.

complementary relationship, temporal scales, wet environment evapotranspiration, Priestley-Taylor equation, state space

The measurement of actual evapotranspiration is important in understanding the hydrologic cycle and in programming and managing water resources. At present, it is difficult to make direct measurement of actual evaporation over large areas. Therefore, indirect estimation models are being utilized in practice. Some of these models are based on the complementary relationship between actual and potential evapotranspiration, such as the complementary relationship areal evapotranspiration model[1], the advection-aridity model[2], and the complementary relationship from unsaturated surfaces[3].

The complementary relationship (CR) between actual and potential evapotranspiration is based on Bouchet hypothesis[4], which states that the decrement in actual evapotranspiration (δE) equals the increment in potential evapotranspiration (δE_p) because of atmospheric feedback on changes in actual evapotranspiration, that is,

$$\delta E = -\delta E_p. \tag{1}$$

The integration of eq. (1) leads to $E+E_p=C$. Wet environment evapotranspiration (E_w) was introduced as a boundary condition. Due to sufficient water supplies at the wet surface, actual evapotranspiration equals both potential and wet environment evapotranspiration. It therefore leads to

$$E + E_p = 2E_w. \tag{2}$$

In complementary relationship models, E_w is usually estimated using the Priestley-Taylor equation[5]:

$$E_w = \alpha \frac{\Delta}{\Delta + \gamma}(R_n - G)/\lambda, \tag{3}$$

where Δ is the slope of saturated vapor pressure versus temperature curve, γ is a psychometric constant, λ is the latent heat of vaporization of water, R_n and G are net radiation and soil heat flux, respectively, and α is a

Received November 7, 2007, accepted June 7, 2008; published online December 8, 2008
doi: 10.1007/s11431-008-0197-3
†Corresponding author (email: yhb99@mails.tsinghua.edu.cn; yangdw@tsinghua.edu.cn)
Supported by the National Natural Science Foundation of China (Grant No. 50509011) and the Major State Basic Research Development Program of China (973 Program) (Grant No.2006CB403405)

parameter (with a standard value of 1.26) that indicates the capacity of available energy (R_n–G) to transform latent heat[6].

In a real catchment system, the impact of advection on CR needs to be taken into consideration. Thus, some studies amended eq. (2) by introducing an advection term[7,8]. Nevertheless, more studies used eq. (3) for estimating E_w and adjusted Priestley-Taylor parameter α instead. This implies the impact of advection. Brutsaert and Chen[9] suggested that α was of the order of 1.26 to 1.28. Hobbins et al.[10] proposed that the α value is within the range of 1.05 to 1.32. Mo[7] took α=1.08 in the North China Plain. Based on the theoretical analysis of the hydrologic and meteorological data obtained from 108 catchments in the inland of China, Yang et al.[11] proposed that α is related to latitude and the distance from ocean and sea due to advection impact, which was explained as a regional variability of CR. Aside from the regional variability, previous studies implied a temporal variability in the CR. When studying the actual evapotranspiration of the Yellow River basin from 1981 to 2000 through the CR model, Liu et al.[12] found that the result had a relatively large error in drought years when choosing a constant α. Using the data from flux measurement stations #40 and #944 from the First International Land Satellite Surface Climatology Field Experiment (FIFE), Pettijohn and Salvucci[13] calibrated α as 1.10 based on the data in July—August from 1987 to 1989, while Szilagyi[14] obtained α as 1.18 (or 1.15) based on the data from station #40 in May—October in 1987 and station #944 in July—August in 1989.

The CR model can estimate actual evapotranspiration over a large region without having to determine underlying surface conditions such as soil moisture. Therefore, it has been widely applied to actual evaporation estimations over different time scales[1,12,15,16], such as monthly[17,18], daily[2], and hourly[19]. In practice, the temporal variability of the CR has an impact on actual evapotranspiration estimation; therefore, further analysis of its regularity and mechanism is required. This paper aims to analyze the variations of α at different time scales and explain the mechanism for these variations.

1 Potential evapotranspiration and wet environment evapotranspiration

This paper adopts the definition of potential evapotranspiration which Penman proposed: in a process an unsaturated surface is brought to saturation, if net radiation, air temperature, and water vapor pressure are held constant, then temperature at the evapotranspiration surface would change and reach a new equilibrium state; evapotranspiration in this new equilibrium state is defined as potential evapotranspiration[15]. Potential evapotranspiration can be calculated using the Penman equation[20]:

$$E_p = \frac{\Delta}{\Delta+\gamma}(R_n - G)/\lambda + \frac{\gamma}{\Delta+\gamma}\cdot 6.43(1+0.536U_2)(p_s - p)/\lambda, \quad (4)$$

where p_s is the saturated vapor pressure (kPa), p is the actual vapor pressure (kPa), and U_2 is the wind speed at the height of 2 m (m/s). Generally, in eq. (4), $\frac{\Delta}{\Delta+\gamma}(R_n - G)/\lambda$ is called the radiative term (R_{rad}), while $\frac{\gamma}{\Delta+\gamma}\cdot 6.43(1+0.536U_2)(p_s - p)/\lambda$ is called the aerodynamic term (R_{aero}).

In a process wherein an unsaturated surface is brought to saturation, if net radiation is held constant, then temperature at the evapotranspiration surface, air temperature, and vapor pressure would change and reach a new equilibrium state; evapotranspiration in this new equilibrium state is defined as wet environment evapotranspiration, and also defined as advection-free potential evapotranspiration[15]. The wet environment evapotranspiration was proposed based on equilibrium evapotranspiration[21], that is, when vapor pressure approaches saturation (p_s–p=0) everywhere above the wet surface, eq. (4) only includes the radiative term, and proportion of latent heat to available energy is $\Delta/(\Delta+\gamma)$, where the equilibrium indicates saturated vapor pressure everywhere[22]. In fact, it is difficult to satisfy the equilibrium condition, and there is even a vapor deficiency above a huge amount of water (such as ocean).Therefore, Priestley and Taylor[5] introduced a coefficient, α, to approach the nonequilibrium state, thus creating the Priestley-Taylor equation. Based on the observations on water and saturated surface, α was taken as 1.26 on average, which was considered as a standard value. The parameter α quantifies the partition of available energy between latent heat (λE) and sensible heat (H), which

can be expressed as

$$\alpha = \left(1+\frac{\gamma}{\Delta}\right)\Big/\left(1+\frac{H}{\lambda E}\right). \quad (5)$$

When sensible heat is downward (i.e. $H < 0$), α will be greater than $1+\gamma/\Delta$; when air is completely saturated above the surface, H and λE change with an identical ratio (i.e. $H/\lambda E = \gamma/\Delta$) and α has a minimum of 1. According to the theory of turbulent diffusion, $H/\lambda E$ can be expressed as a function of vapor pressure difference (Δp) and temperature difference (Δt) between surface and reference height, as shown by the following equation:

$$H/\lambda E = \gamma\frac{\Delta t}{\Delta p}. \quad (6)$$

Substitution of eq. (6) into (5) yields

$$\alpha = \left(1+\frac{\gamma}{\Delta}\right)\Big/\left(1+\gamma\frac{\Delta t}{\Delta p}\right). \quad (7)$$

Compared to the condition without advection, the horizontal transport of heat and water vapor by advection will affect Δp and Δt, and eventually α.

2 Analysis of temporal variations of the CR

2.1 Data and method

In order to analyze the annual variability of the CR, this study selected 38 catchments in the Haihe River basin with drainage areas of 272—25500 km^2. The hydrologic and meteorological data were collected from each catchment from 1953—1998. Figure 1 presents the distribution of hydrologic and meteorological stations in the study region. The procedures for catchment areal average precipitation and potential evapotranspiration were as follows: (1) A 10-km grid data set covering the study region was interpolated from 54 meteorological stations in the study region and the area surrounding it. (2) Potential evapotranspiration was estimated in each grid. (3) The areal average values for each catchment were calculated. Air temperature was interpolated using an inverse distance weighted technique, taking into consideration the impact of elevation. Other variables were interpolated using an inverse distance weighted technique. For more details about the data and methods, see refs. [23, 24].

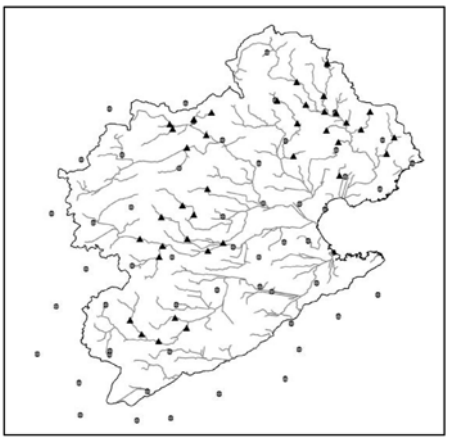

Figure 1 Distribution of the hydrologic and meteorological stations in the Haihe River basin (the solid circles represent meteorological stations and the solid triangles represent hydrologic stations).

To study the temporal variability of the CR within small time scales, data from the Weishan experiment site (36°39′N, 116°03′E, elevation of 30 m)[25] located in the irrigation district along the down stream of the Yellow River were obtained from May 18, 2005 to December 31, 2006. The variables observed included normal meteorological variables, net radiation flux, latent heat flux, sensible heat flux, and soil heat flux, among others. Latent heat and sensible heat fluxes were observed using the eddy correlation technique. Data were recorded every 30 min on the average. The energy balance enclosure was about 80%.

Substitution of eq. (3) into eq. (2) leads to the equation for estimating the parameter α, as follows:

$$\alpha = \frac{1}{2}\left(\frac{E_p + E}{E_{rad}}\right). \quad (8)$$

where E_{rad} is the radiative term, which can be expressed as $E_w = \alpha E_{rad}$.

2.2 Variation of the CR on different time scales

2.2.1 Inter-annual variation. On annual scale, the annual α value of 38 catchments was calculated using eq. (8), after which, the mean, maximum, and minimum values of α for each catchment were obtained (see Figure 2(a)). On the other hand, the α value for each catchment, based on the mean annual E_p, E, and E_{rad}, was used to calculate the annual actual evapotranspiration (E_{cal}) using the equation $E=2E_w-E_p$. The relative error was evaluated according to the equation $|(E_{cal}-E)/E_{cal}|\times 100\%$. Figure 2(b) illustrates the probability that the absolute value of the relative error is larger than

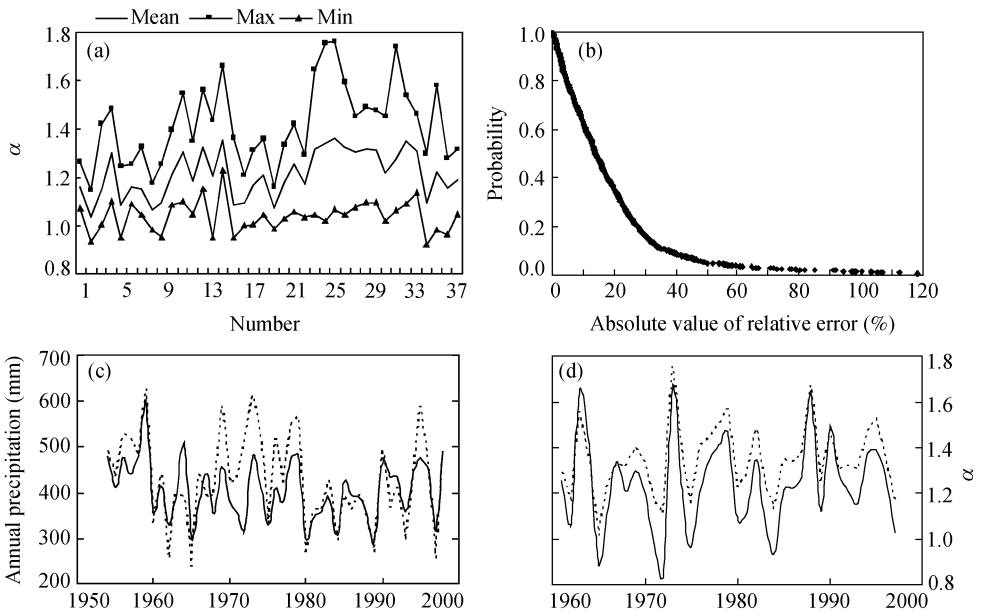

Figure 2 (a) Mean, maximum, and minimum values of α for each catchment; (b) absolute value of the relative error between the estimated E and observed E (including 1317 data points); (c) and (d) the inter-annual variation in precipitation and α for the two catchments, respectively (the dot represents annual precipitation and the dash represents α).

a special value. Figures 2(c) and 2(d) demonstrate the inter-annual variation of precipitation and α for the two catchments.

Figure 2(a) shows that α has large inter-annual variations, with values ranging from 0.74 to 0.17. Figure 2(b) shows that a large error will be incurred in estimating the actual evapotranspiration based on the CR if the inter-annual variation of α will not be taken into consideration. It likewise shows that the error in 60% of the results is greater than 10%, while in 35% of the results, the error is larger than 20%. Figures 2 (c) and 2(d) show an in-phase change between α and P.

2.2.2 Seasonal variation. Based on the data from the Weishan experiment site, the seasonal variation of the CR has been studied. We estimated the daily average of E_p, E, and E_{rad}, and calculated the average every 10 days. After this period, the value for α was calculated using eq. (8), which was then plotted in Figure 3(a). In contrast, the annual mean of α was estimated at 1.32 based on the annual means of E_p, E, and E_{rad} (i.e. the sum of their daily value). The actual evapotranspiration for every 10 days (E_{cal}) was then calculated using the equation $E = 2E_w - E_p$. The comparison of E_{cal} with the observation of actual evapotranspiration is shown in Figure 3(b).

Figure 3(a) shows a significant seasonal variation in parameter α, which was larger in winter than in summer.

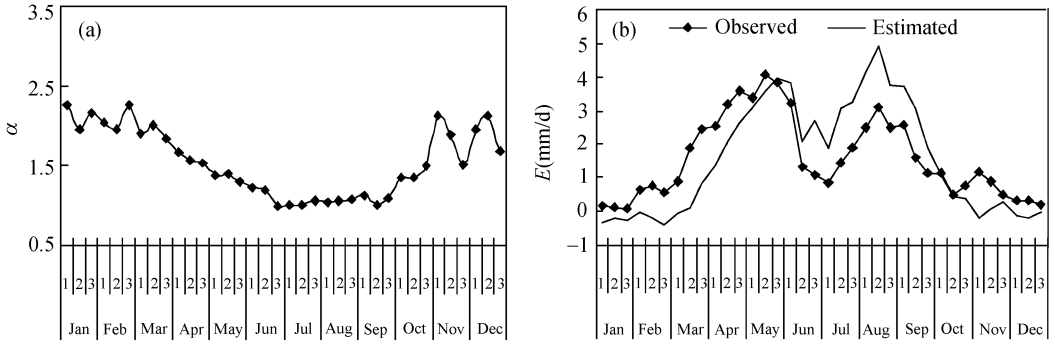

Figure 3 (a) Seasonal variation in α; (b) comparison of actual evapotranspiration E between the estimated (neglecting seasonal variation in α) and the observed values.

As shown in Figure 3(b), the actual evapotranspiration estimated by the CR has a relatively large error if the seasonal variability of α is not taken into consideration. From January to mid-May and from mid-October to December, the calculated actual evapotranspiration is smaller than what is actually observed, and the maximum error is –1.8 mm/d in mid-March. During the other seasons, the calculated value is larger than the observed value, and the maximum error is 1.8 mm/day in mid-August.

2.2.3 Daily variation. The time range was limited to 08:00—16:00 in this study. Based on the data from the Weishan experiment site in 2006, α for every 30 min was estimated and then calculated for the annual mean of intra-daily variation (one value for every 30 min) (see Figure 4(a)). On the other hand, using the annual E_p, E, and E_{rad}, the annual mean of α was estimated as 1.05. This was different from the 1.32 value in the previous section because this data only covered the range of 8:00—16:00 in this section. The actual evapotranspiration (E_{cal}) for every 30 min was then estimated using the equation E=2E_w–E_p, as shown in Figure 4(b). Figure 4(a) also demonstrates that α has a downward trend at forenoon and an upward trend in the afternoon, and the average α value is smaller in the morning than in the afternoon. Figure 4(b) shows that the actual evapotranspiration estimated by the CR has a relatively large error if the seasonal and intra-daily variations of α are neglected. From 08:30—13:30, the calculated actual evapotranspiration is larger than the observed value, with a maximum error (0.027 mm/30 min) at 11:30; at 08:00 and from 14:00—16:00, the calculated value is smaller than the observed value, with a maximum error (–0.055 mm/30 min) at 16:00.

3 Analysis of the mechanism of temporal variations

3.1 Illustration of the advection impact in the vapor pressure-temperature (*p-t*) state space

The impact of advection on wet environment evapotranspiration was analyzed in the vapor pressure-temperature (*p-t*) state space, which was revealed through the variation in α. The energy balance equation can be expressed as

$$R_n - G = \lambda E + H, \tag{9}$$

where the relationship among available energy (R_n–G), latent heat (λE), and sensible heat (H) can be illustrated through *p-t* state space[26]. Based on the state space, Eagleson[6] illustrated the concept of wet environment evapotranspiration (see Figure 5). In Figure 5, $p_s(t)$ is the saturated vapor pressure-temperature curve, which is close to a line (BC) when the temperature only undergoes a narrow change. Line BD describes a change process with constant vapor pressure, whose slope is the slope of saturated vapor pressure-temperature curve, Δ. Therefore, the angle $\angle CBD$ can be expressed as $\tan^{-1}\Delta$. Line AC represents an isothermal process. Line BF represents an adiabatic change process, whose slope is γ. The angle $\angle DBA$ can thus be measured as $\tan^{-1}\gamma$. Reaching an equilibrium state at wet environment, the temperature difference between surface and reference height is very small. Therefore, it is assumed that the states adjacent to the wet surface and at reference height

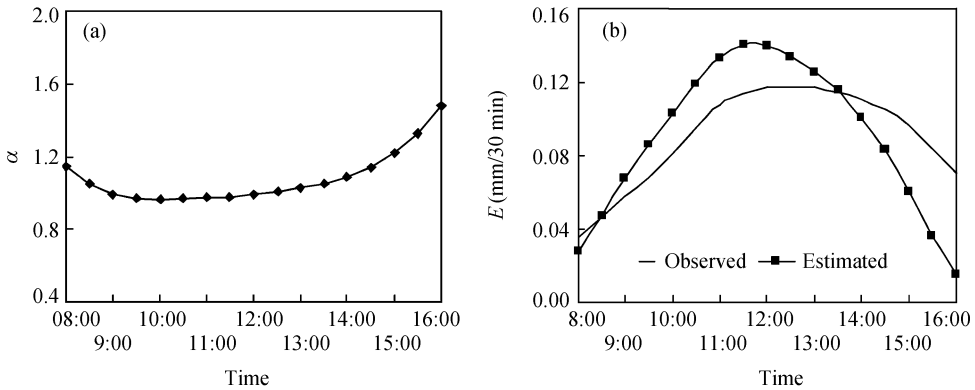

Figure 4 (a) Annual mean of daily variation in α; (b) comparison of actual evapotranspiration E between the estimated (neglecting seasonal and daily variations in α) and the observed.

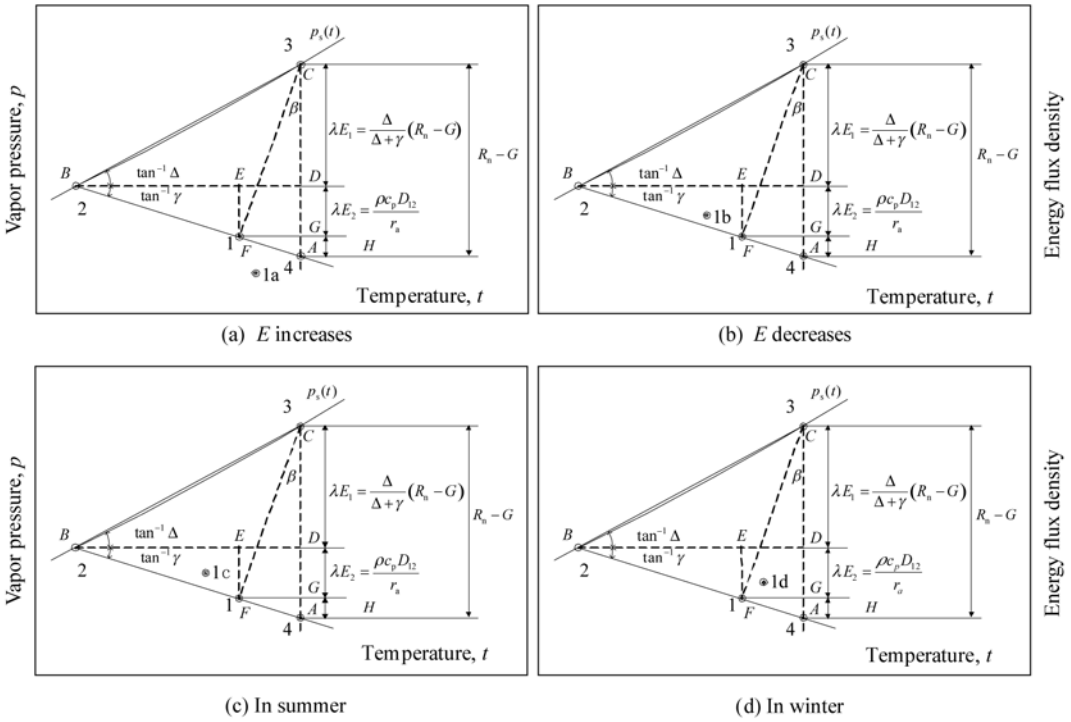

Figure 5 Impact of actual evapotranspiration and seasonal variations on the complementary relationship.

can be represented by Points 3 and 1 respectively, in the state space. According to the First Law of Thermodynamics, the path from one point to another through the *e*-*T* state space is arbitrary, and only the end states matter. Therefore, the change from Points 1 to 3 can be divided into two sub-processes (i.e. the change sub-process along the curve $p_s(t)$ and an adiabatic change sub-process). In the former sub-process, the latent heat flux is $\lambda E_1 = \Delta/(\Delta+\gamma)\cdot(R_n - G)$; in the latter, the increment of latent heat equals the decrement of sensible heat $\rho c_p(T_1 - T_2) = \rho c_p D_{12}$ (where ρ is the density of air and c_p is the specific heat of air), and the latent heat flux equals the rate between the increment of latent heat and the atmospheric resistance r_a (i.e. $\lambda E_2 = \rho c_p D_{12}/r_a$). Nevertheless, wet environment evapotranspiration can be expressed as

$$E_w = E_1 + E_2 = \frac{\Delta}{\Delta+\gamma}(R_n - G)/\lambda + \frac{\rho c_p D_{12}}{r_a \lambda}. \quad (10)$$

Assuming $k = L_{BE}/L_{BD}$ (L_{BE} representing the length of Line *BE*, as well as others), according to the geometric relation in Figure 5, we can obtain

$$\tan\beta = \frac{L_{FG}}{L_{CG}} = \frac{L_{ED}}{L_{CD}+L_{DG}} = \frac{L_{BD}(1-k)}{L_{BD}\Delta + L_{BD}\gamma k} = \frac{1-k}{\Delta+\gamma k}. \quad (11)$$

The parameter α of the Priestley-Taylor equation can be expressed as

$$\alpha = \frac{L_{DG}+L_{CD}}{L_{CD}} = \frac{L_{EF}+L_{CD}}{L_{CD}} = \frac{k\gamma L_{BD} + \Delta L_{BD}}{\Delta L_{BD}} = \frac{k\gamma}{\Delta} + 1. \quad (12)$$

Substitution of eq. (11) into (12) yields

$$\alpha = \frac{\gamma}{\Delta}\cdot\frac{1-\Delta\tan\beta}{1+\gamma\tan\beta} + 1. \quad (13)$$

According to eq. (13), when β equals 0, $\alpha = 1+\gamma/\Delta$, evapotranspiration is an isothermal process (i.e. the temperatures at wet surface and reference height are identical), and $H = 0$. Under some special conditions, it is possible that $\beta < 0$, $\alpha > 1+\gamma/\Delta$, and $H < 0$. When $\Delta\tan\beta = 1$, α has a minimum of 1, which indicates that water vapor is saturated everywhere and the dry power of atmosphere is 0. The relationship $H/\lambda E = \gamma/\Delta$ can therefore be obtained.

3.2 Mechanism of inter-annual variation in parameter α

On annual scale, the increase in precipitation *P* leads to the increase in actual evapotranspiration *E*. This will modify the atmospheric state and result in heightening vapor pressure and lowering temperature. Assuming that the land-atmosphere system is a closed system that does not undergo any exchange of heat and water vapor with

its external environment, Point 3 represents the state (i.e. vapor pressure and temperature) at the wet surface and Point 1 represents the state at the reference height. As an open land-atmosphere system, a real catchment weakens the effect of changing E on vapor pressure and temperature. In other words, relative to the state in a closed system, vapor pressure decreases and temperature increases when E increases. Hence, the point representing the state at reference height will move from Point 1 to Point 1a (see Figure 5(a)). When vapor pressure increases and temperature decreases when E decreases, the point representing the state at reference height will move from Point 1 to Point 1b (see Figure 5(b)). The variation in state at the wet surface (i.e. Point 3) can be neglected because advection has less effect on the state at the wet surface than it does at the reference height. In the state space, as shown in Figure 5, β decreases with an increase in E, while β increases with a decrease in E. According to eq. (13), the parameter α of P-T equation and E changes in phase. In some catchment, E increases with an increase in P, thus α and P have a variation in phase. In 28 catchments of the Haihe River basin, the correlation coefficient between P and α is larger than 0.8, whose distribution is shown in Figure 6, without significant regional characteristics.

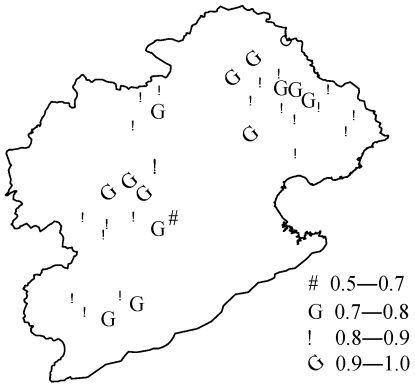

Figure 6 Distribution of the correlation coefficient between precipitation (P) and α.

3.3 Mechanism of seasonal variation in α

Seasonal variation in α was due to the difference in thermodynamic property between continent and ocean and the regional variation in solar radiation. Possessing a large heat capacity, the ocean absorbs heat during summer and releases heat during winter, consequently adjusting the temperature of the atmosphere above it. Relative to above ocean, during summer, the atmosphere above continent has less water vapor content and higher temperature, such that advection results in vapor pressure heightening and temperature lowering. On the other hand, in winter, the atmosphere has less water vapor content and lower temperature, such that advection leads to a rise in both vapor pressure and temperature. Runoff from continent to ocean is relevant to the vapor transport by advection from ocean to continent. The distribution of isothermal lines, that is, temperature having an inverse relationship with the distance from ocean at identical latitude regions, indicates the phenomenon that heat is being transported from ocean to continent by advection. As a result, the state at the reference height moves from Point 1 (representing the state without advection) to Point 1c in Figure 5(c) in summer; movement is observed from Point 1 to Point 1d in Figure 5(d) in winter. This results in β decreasing in summer and increasing in winter. Neglecting state changes at the wet surface (represented by Point 3), according to eq. (13), the seasonal variation in α is greater in winter and less in summer.

3.4 Mechanism of daily variation in α

Solar radiation has a marked daily variation, and the radiative term E_{rad} has a consistent variation. The aerodynamic term E_{aero} is related to atmospheric state (temperature and relative humidity, among others), whose daily variation has a smaller amplitude than solar radiation does and has a lag in phase. The atmospheric response to surface changes is hysteric. For example, maximum air temperature comes later than maximum surface temperature (see Figure 7(a)). Therefore, during forenoon, which is accompanied by intensifying solar radiation, E_{rad} and E_{aero} increase, however E_{aero} exhibits less change than E_{rad} does. In the afternoon, due to the waning of solar radiation, E_{rad} decreases, while E_{aero} initially increases and then decreases at a value less than E_{rad} (see Figure 7(b)). Nevertheless, $E_{\mathrm{aero}}/E_{\mathrm{rad}}$ decreases in the forenoon and increases in the afternoon, and the resulting average in the forenoon is less than that in the afternoon. On intra-daily time scale, the relationship of actual evapotranspiration E with potential evapotranspiration E_{p} can be expressed as $E = k_s E_{\mathrm{p}}$, where k_s is a parameter relating to surface condition and with a little variation (see Figure 7(c)). Substitution of $E = k_s E_{\mathrm{p}}$ into eq. (8) yields $\alpha = \frac{1}{2}\left[E_{\mathrm{p}} + k_s E_{\mathrm{p}}\right] \Big/ E_{\mathrm{rad}} = \frac{1}{2}[1 + k_s] E_{\mathrm{p}} /$

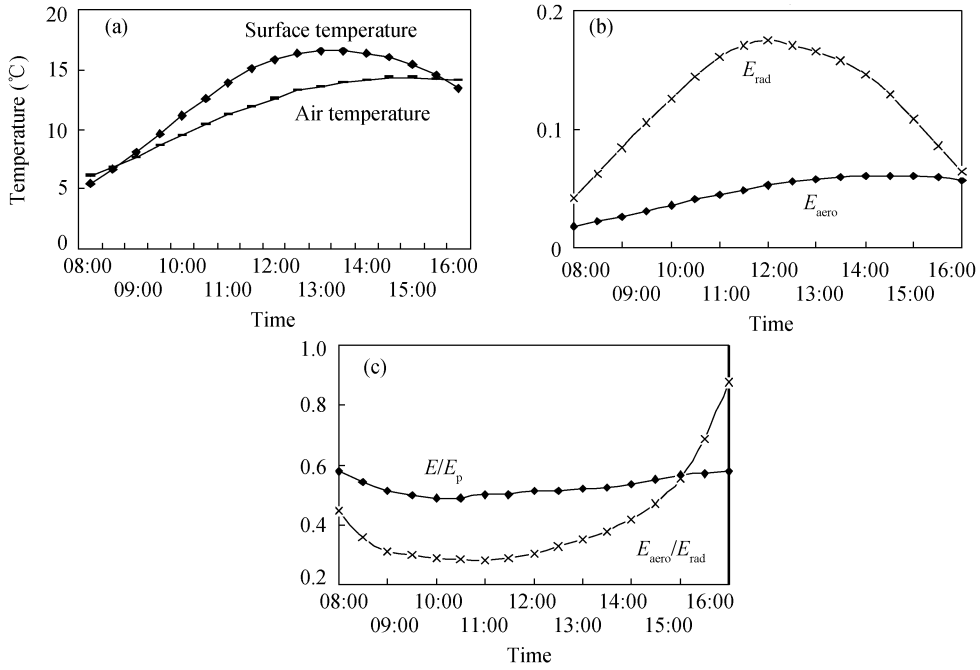

Figure 7 Daily variations in: (a) surface temperature and air temperature; (b) E_{rad} and E_{aero}; and (c) E_{aero}/E_{rad} and E/E_p.

$E_{rad} = \frac{1}{2}[1+k_s](1+E_{aero}/E_{rad})$. Neglecting the variation in k_s, decreasing E_{aero}/E_{rad} leads to the decrease of α in the forenoon, while α increases as a result of increasing E_{aero}/E_{rad} (see Figure 7(c)). On the average, E_{aero}/E_{rad} is less in the forenoon than in the afternoon. Therefore, α has a consistent variation.

4 Conclusions

Based on the data obtained from 38 catchments of the Haihe River basin and the Weishan experiment site located in the irrigation district of Shandong Province in China, the variations in the complementary relationship on different time scales were revealed. Through theoretical and data analyses, this study drew the following conclusions: (1) For estimating the actual evapotranspiration, the variability of the complementary relationship at different time scales needs to be considered. (2) Evapotranspiration changes have an impact on the atmospheric state, which is weakened in an open atmosphere system, resulting in an inter-annual variability (i.e. larger α in the year with greater periods of precipitation). (3) The transport of water vapor and heat between ocean and continent brings about a seasonal variability of the CR (i.e. α has a larger value in winter than in summer). (4) On an hourly scale, atmospheric feedback to the change in actual evapotranspiration is hysteretic, resulting in a daily variability of the CR (i.e. α increasing in the forenoon and decreasing in the afternoon, and having a lower mean value in the forenoon than in the afternoon).

In this paper, we performed a heuristic study on the variation of the CR; further quantitative analysis is needed. As a makeshift method, α values can be determined when estimating actual evapotranspiration on different time scales respectively, such as different values corresponding to different annual precipitation (i.e. wet year, normal year or dry year), different values for various seasons, and different values for forenoon and afternoon.

1 Morton F I. Estimating evapotranspiration from potential evaporation: practicality of an iconoclastic approach. J Hydrol, 1978, 38: 1－32
2 Brutsaert W, Stricker H. An advection-aridity approach to estimate actual regional evapotranspiration. Water Resour Res, 1979, 15(2): 443－450
3 Granger R J. An examination of the concept of potential evaporation, 1989, J Hydrol, 111: 9－19
4 Bouchet R. Evapotranspiration reelle at potentielle, signification climatique. IAHS Publication, 1963, 62: 134－142
5 Priestley C H B, Taylor R J. On the assessment of surface heat flux and evaporation using large-scale parameters. Monthly Weather Rev, 1972, 100(2): 81－92

6 Eagleson P S. Ecohydrology: Darwinian Expression of Vegetation Form and Function. Cambridge: Cambridge University Press, 2002
7 Mo X G. An advection-aridity evaporation model for wheat field evapotranspiration and advection (in Chinese). Agric Meteorol, 1995, 16(6): 1－4
8 Morton F I. Estimating evaporation and transpiration from climatological observations. J Appl Moteorol, 1975, 14: 488－497.
9 Brutsaert W, Chen D. Desorption and the two stages of drying of natural tallgrass prairie. Water Resour Res, 1995, 31: 1305－1313
10 Hobbins M T, Ramı´rez J A, Brown T C. The complementary relationship in estimation of regional evapotranspiration: An enhanced advection-aridity model. Water Resour Res, 2001, 37: 1389－1403
11 Yang H B, Yang D W, Lei Z D, et al. Regional variability of the complementary relationship between actual and potential evapotranspiration. J Tsinghua Univ (Sci & Tech), 2007, 48(9): 1409－1412
12 Liu S M, Sun R, Sun Z P, et al. Comparison of different complementary relationship models for regional evapotranspiration estimation (in Chinese). Acta Geogr Sin, 2004, 59(3): 331－340
13 Pettijohn J C, Salvucci G D. Impact of an unstressed canopy conductance on the Bouchet-Morton complementary relationship. Water Resour Res, 2006, 42: W09418, doi:10.1029/2005WR004385
14 Szilagyi J. On the inherent asymmetric nature of the complementary relationship of evaporation. Geophys Res Lett, 2007, 34: L02405, doi:10.1029/2006GL028708
15 Qiu X F, Zeng Y, Miao Q L, et al. Estimation of annual actual evapotranspiration from nonsaturated land surfaces with conventional meteorological data. Sci China Ser D-Earth Sci, 2004, 47(3): 239－246
16 Xu X K, Sui H Z, Tian G L. Application and research of complementary relationship theory in remote sensing (in Chinese). J Remote Sens, 1999, 3(1): 54－59
17 Morton F I. Climatological estimates of evapotranspiration. J Hydraul Div Proc ASCE, 1976, 102: 275－291
18 Morton F I. Operational estimates of areal evapotranspiration and their significance to the science and practice of hydrology. J Hydrol, 1983, 66: 1－76
19 Parlange M B, Katul G G. An advection-aridity evaporation model. Water Resour Res, 1992, 28: 127－132
20 Penman H L. Natural evaporation from open water, bare soil and grass. Proc Roy Soc London, 1948, A193: 120－146
21 Slatyer R O, McIlroy I C. Evaporation and the principle of its measurement. In: Practical Meteorology. CSIRO (Australia) and UNESCO, Paris, 1961
22 Culf A D. Equilibrium evaporation beneath a growing convective boundary layer. Boundary-Layer Meteorol, 1994, 70: 37－49
23 Yang D, Sun F, Liu Z, et al. Analyzing spatial and temporal variability of annual water-energy balance in non-humid regions of China using the Budyko hypothesis. Water Resour Res, 2007, 43: W04426, doi: 10.1029/2006WR005224
24 Sun F B, Yang D W, Liu Z Y, et al. Study on coupled water-energy balance in Yellow River basin based on Budyko Hypothesis (in Chinese). J Hydraul Eng, 2007, 38(4): 27－35
25 Lei H M, Yang D W, Shen Y J, et al. Energy and water fluxes in the Yellow River irrigation region (in Chinese). J Tsinghua Univ (Sci & Tech), 2007, 47(6): 801－804
26 Monteith J I. Evaporation and environment. Symp Soc Exp Biol, 1965, 19: 205－234